*remote sensing*

MDPI

*Communication*

# Winds of Change for Future Operational AMV at EUMETSAT

**Régis Borde [1,*], Manuel Carranza [2], Olivier Hautecoeur [3] and Kevin Barbieux [1]**

1 EUMETSAT, 64295 Darmstadt, Germany; kevin.barbieux@eumetsat.int
2 GMV INSYEN, 82234 Weßling, Germany; manuel.carranza@external.eumetsat.int
3 EXOSTAFF, 64404 Bickenbach, Germany; olivier.hautecoeur@external.eumetsat.int
* Correspondence: regis.borde@eumetsat.int

Received: 30 July 2019; Accepted: 6 September 2019; Published: 10 September 2019


**Abstract:** EUMETSAT, the European Organization for the Exploitation of Meteorological Satellites, is one of the key contributors to global atmospheric motion vector (AMV) production around the world. Its current contribution includes geostationary satellites at 0.0 and 41.5 degrees east, and several products extracted from the Metop low-orbit satellites. These last ones mainly cover high-latitude regions completing the observations from the geostationary ring. In the upcoming years, EUMETSAT will launch a new generation of geostationary and low-orbit satellites. The imager instruments Flexible Combined Imager (FCI) and METImage will take over the nominal AMV production at EUMETSAT around 2022 and 2024. The enhanced characteristics of these new-generation instruments are expected to increase AMV production and to improve the quality of the products. This paper presents an overview of the current EUMETSAT AMV operational production, together with a roadmap of the preparation activities for the new generation of satellites. The characteristics of the upcoming AMV products are described and compared to the current operational AMV products. This paper also presents a recent investigation into AMV extraction using the Sentinel-3 Sea and Land Surface Temperature Radiometer (SLSTR) instrument, as well as the retrieval of wind profiles from infrared sounders.

**Keywords:** Atmospheric Motion Vectors (AMVs); MSG; EPS; MTG; EPS-SG; wind profile; Infra-red sounders

## 1. Introduction

The improvement of numerical weather prediction (NWP) forecast models requires the near-real-time assimilation of meteorological observations that inform the models about the current state of the atmosphere. Therefore, NWP models are continuously fed with a wide range of in-situ observations, like radiosondes, radars, buoys, aircraft measurements, and observations extracted from satellite data. The proportion of satellite data assimilated in NWP models has increased a lot during recent years because these models cover all areas around the Earth, including the oceans and the polar regions, where few in-situ measurements are available [1]. Atmospheric motion vectors (AMV) derived by tracking clouds or water-vapor features in consecutive satellite images, constitute the only upper-level wind observations with good global coverage that help to predict the evolution and displacement of air masses. As mentioned in the final report of the sixth World Meteorological Organization (WMO) Workshop on the Impact of Various Observing Systems on Numerical Weather Prediction held on 10–13 May 2016 at the Shanghai Meteorological Service in China, AMVs are in the top five of observing systems contributing to the forecast performance of global NWP models [2]. The impact of AMVs on forecast performance has increased during the last few years due to the

larger amount of AMVs produced, better AMV characterization, and the better use of AMVs in the assimilation processes.

At the European Organization for the Exploitation of Meteorological Satellites (EUMETSAT), AMVs are operationally derived from both geostationary and low-Earth-orbit satellites. The hourly AMV product extracted from Meteosat Second Generation (MSG) is an average of three intermediate vectors calculated from a sequence of four consecutive Spinning Enhanced Visible and InfraRed Imager (SEVIRI) images that observe the full Earth disk every 15 min [3]. AMVs are derived from two visible channels (VIS0.8 and High-Resolution Visible, HRVIS), two water-vapor channels (WV6.2 and WV7.3), and one infrared channel (IR10.8). The spatial resolution at nadir is 3 km for all SEVIRI channels except the HRVIS channel, where it is 1 km, allowing for the retrieval of smaller scale motions. The primary service, Full Earth Scan (FES) at 0° every 15 min, has been provided by the *Meteosat-11* satellite since April 2018, with *Meteosat-10* performing the Rapid Scan Service (RSS) over Europe. The operations over the Indian Ocean have been ensured by the *Meteosat-8* satellite at 41.5° east since February 2017.

AMVs have also been derived over polar regions since 2011 using data from the Advanced Very High-Resolution Radiometer (AVHRR/3) onboard the Metop satellites. The latest version of the AVHRR AMV extraction algorithm developed in 2015 allows for the extraction of three different AVHRR AMV products [4,5], using either a pair or a triplet of AVHRR images taken from one or two Metop satellites with different coverage and temporal gaps between successive images in order to extract cloud motions. The assimilation of global AVHRR wind products [6] in NWP models has shown a positive impact on the forecast scores at several meteorological agencies: ECMWF, DWD, MET Norway, and the United States Navy Fleet Numerical Meteorology and Oceanography Center (FNMOC). The main benefit of these products occurs in high-latitude areas, especially in the 40–60 degrees latitude band, where few wind observations are usually available for assimilation.

Launched in 2006, the *Metop-A* satellite started to drift in its orbit in August 2018 in order to slowly prepare its end of operational lifetime. Since the launch of *Metop-C* in October 2018, data from the three Metop satellites have been processed at EUMETSAT, and they can be used for operations until the decommissioning of *Metop-A*. A tristar configuration (a phasing of 120 degrees between each pair of satellites) of the three Metop satellites has been decided for the commissioning of *Metop-C*, potentially providing operations until 2021. Single AVHRR wind products are now extracted from all *Metop-A*, *Metop-B* and *Metop-C* satellites over the polar regions. It was necessary to adapt the algorithm for the production of dual-satellite AVHRR AMVs to this new configuration and to study its potential benefits. Since 17 January 2019, the dual operation of Metop satellites has produced AMVs from three combinations of images: *Metop-A*/*Metop-B*, *Metop-B*/*Metop-C*, and *Metop-C*/*Metop-A* [7].

In summary, as illustrated in Figure 1, the current EUMETSAT contribution to global AMV production encompasses the MSG geostationary disks at 0.0 and 41.5 degrees east, the northern and southern high-latitude (poleward of 50 degrees) areas with the *Metop-A*, *Metop-B* and *Metop-C* single AVHRR wind products, and global coverage using the global AVHRR wind products. The pictures represent the AMV observations used at ECMWF for the 1 July 2019 midnight model run.

Both MSG and Metop EUMETSAT programs are approaching their end, and several significant changes are planned for the upcoming years to ensure the continuity of the current EUMETSAT operation capabilities with the new programs. The deployment of the Meteosat Third Generation (MTG) system will start with the launch of the first imaging satellite, *MTG-I1*, planned in the second half of 2021. MTG-I will continue and enhance the imaging service currently provided by MSG using the Flexible Combined Imager (FCI) data. The development of the MTG/FCI algorithms has already started at EUMETSAT based on the MSG code in order to verify the product/quality of the industry-provided operational codes. In addition, an extended scientific validation of AMVs will be performed with the next generation of geostationary satellite AMVs (*Himawari-8/-9*, *GOES-R* and *GeoKompsat*), which have similar characteristics to those of the MTG/FCI instrument.

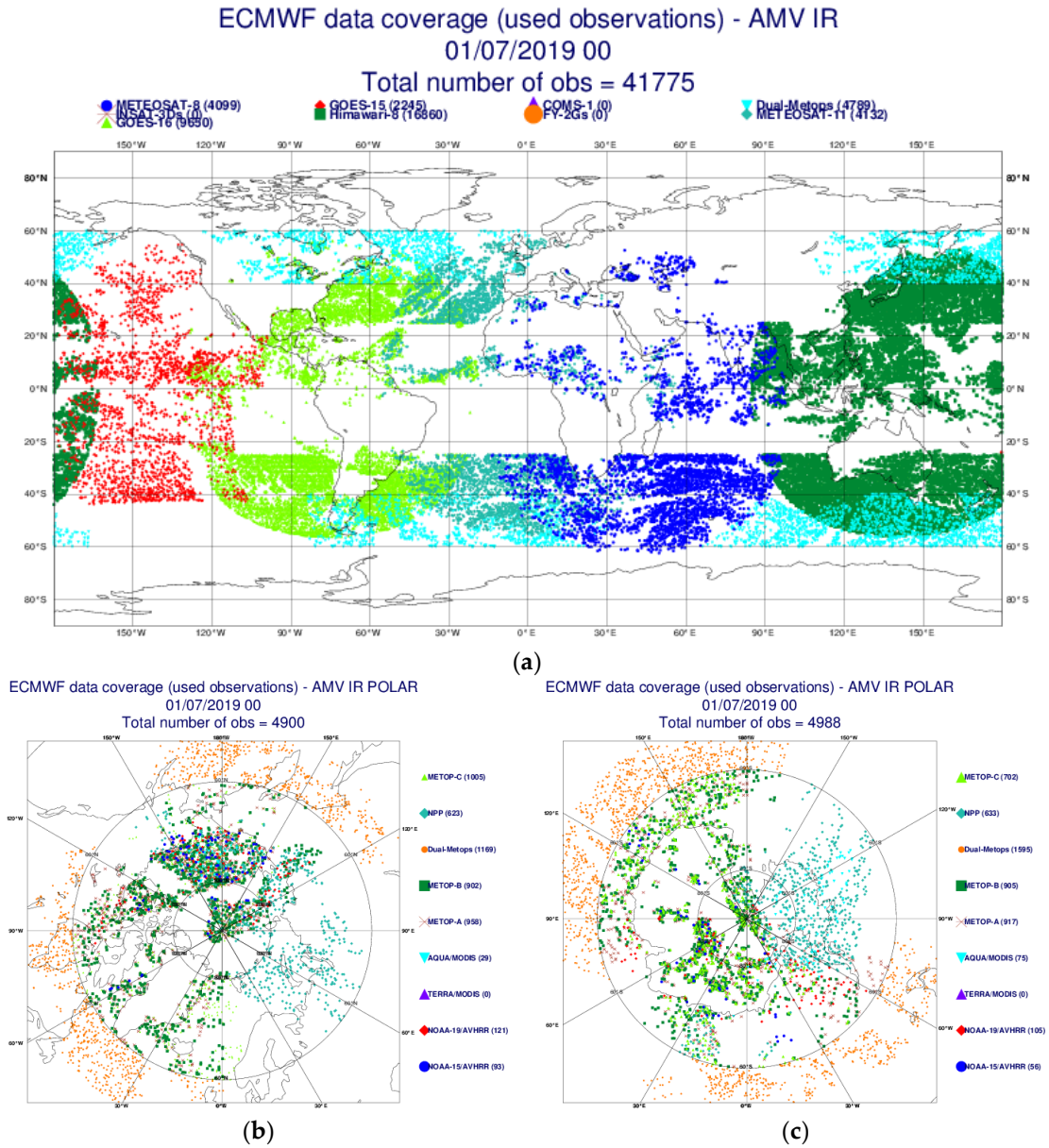


**Figure 1.** Illustration of European Organization for the Exploitation of Meteorological Satellites (EUMETSAT)'s contribution to the global atmospheric motion vector (AMV) production system over the geostationary satellite ring, with *Meteosat-11* (dark turquoise) and *Meteosat-8* (dark blue), and dual Advanced Very High-Resolution Radiometer (AVHRR) (cyan) AMV products (**a**) and over the northern (left) and southern (right) polar areas with *Metop-A* (red crosses), as well as the *Metop-B* (dark green) and *Metop-C* (light green) single and global AVHRR (orange) wind products (**b**). Images downloaded from ECMWF satellite data monitoring website for the 1 July 2019 at 00:00 UTC. Please note that the gap of data in the tropics in Figure 1a is due to the blacklisting filter used in assimilation process at ECMWF and not due to a lack of satellite data.

The current EUMETSAT Polar System (EPS) will be replaced in the early 2020s by the so-called EPS Second Generation (EPS-SG). AMVs over the polar areas will then be extracted from the optical imager METImage on board the first Metop-SG satellite. The METImage instrument is a cross-track-scanning imaging spectro-radiometer which measures reflected solar and emitted terrestrial radiation in the visible-to-infrared spectral domain between 0.445 and 13 µm with a moderate sampling resolution of 0.5 km. METImage will simultaneously provide images in 20 spectral channels, allowing for the

extraction of AMV in the visible (0.8 µm), infra-red (10.7 µm) and water vapor (6.7 and 7.3 µm) channels, making the AMV extraction very similar to that from the MSG/SEVIRI and MTG/FCI instruments. The extraction of water-vapor winds from Low Earth Orbit (LEO) satellites over polar areas is presently ensured by the Moderate-Resolution Imaging Spectroradiometer (MODIS) instrument on board the NASA EOS-TERRA and EOS-AQUA missions [8]. This is a high-level requirement from the user community, and METImage is expected to take over the water-vapor wind production over polar areas after 2022. The launch of *Metop-SG-A1* is currently planned for 2022, and the algorithm prototyping activities for the METImage instrument are presently taking place at EUMETSAT using the algorithm baseline developed for MTG/FCI. The scientific validation is planned to be performed against similar polar-wind products extracted from MODIS, the Visible Infrared Imaging Radiometer Suite (VIIRS) and the AVHRR.

Though AMVs have a significant impact on forecast error reduction, their extraction depends on the presence of clouds, and it provides information at a single level in the atmosphere. Therefore, they cannot entirely fulfil the user requirements defined for the horizontal wind parameter in the WMO Observing System Capability Analysis and Review (OSCAR) database (https://www.wmo-sat.info/oscar/): A horizontal resolution of about 50 km and vertical resolution of about 1 km for global NWP applications. Vertical wind profiles are presently provided by the conventional radiosonde network, by the radar Doppler network, and from ascent and descent wind profiles from civil aircraft [9]. They can also be measured by Doppler lidar instruments like the European Space Agency (ESA) Aeolus mission that was launched in August 2018. Despite the critical user requirement of observed wind profiles, an operational Aeolus follow-on mission is still under discussion and has not been decided yet—it is awaiting the demonstration of Aeolus in space and its impact on forecast scores. Even if an operational Aeolus mission is decided, the period needed to build the satellite and get the operational production of wind profiles is estimated to last around a decade.

3D wind profiles can, in theory, also be extracted from infrared sounder instruments that provide vertically resolved observations of humidity fields. A horizontal wind profile product was part of the initial Meteosat Third Generation InfraRed Sounder (MTG/IRS) user requirements, but it was then classified as an 'aspirational product' due to the low maturity level of the products at the time [10]. During the last 15 years, several studies in Europe and the United States of America have demonstrated the feasibility of multi-layer wind-field extraction from humidity fields derived from hyperspectral sounders [11–13]. A demonstration product is currently produced at Cooperative Institute for Meteorological Satellite Studies (CIMSS) using data from the Atmospheric InfraRed Sounder (AIRS) flying on board AQUA [13]. The overlapping between consecutive AIRS images allows for wind extraction only at high latitudes poleward of 70 degrees. The overall forecast impact of this product was deemed neutral in the Goddard Earth Observing System Model version 5 (GEOS-5) model, but the impact per observation has been found to be very good for AIRS moisture AMVs [13]. A 3D optical-flow scientific processor has been recently developed at EUMETSAT to extract wind profiles from IR sounders. This processor is based on an algorithm that initially worked with three layers of cloud-top height information [14] and that has been modified to ingest the Infrared Atmospheric Sounding Interferometer (IASI) level 2 humidity information. Wind profiles are retrieved from pairs of IASI datasets taken by the *Metop-A* and *Metop-B* satellites over high-latitude areas [15]. Though in a preliminary stage, the first results look very promising, providing dense wind fields at several levels in the atmosphere over the areas covered by the Metop/IASI instrument poleward of 45 degrees.

Section 2 of this paper presents the current status and recent changes in the operational AMV production capabilities at EUMETSAT. Section 3 gives an overview of the last developments foreseen for the near future. Emphasis is given on the benefits on the AMV extraction that are expected from the new generations of geostationary and polar-orbiting satellites that will be operated by EUMETSAT in the upcoming years.

## 2. Recent Changes in the Operational AMV Production at EUMETSAT

### *2.1. MSG/SEVIRI AMV Products*

Since 2008, a coordinated effort has been organized to compare the AMV products extracted by different AMV producers. This has resulted so far in a total of three intercomparison studies which have assessed how the satellite-derived cloudy AMVs compare in terms of coverage, speed, direction and altitude. The first two AMV intercomparison studies took place in 2008 and 2014 [16–18]. The third AMV intercomparison study, which took place in 2018, included a test using a common quality index (QI) by all the participants [19]. The use of a common QI has proven being very useful in filtering collocated AMVs resulting in an improved statistical agreement. Both working groups I (data production) and II (data assimilation) at the Fourteenth International Wind Workshop (IWW14) encouraged the implementation of a so-called common QI within all the operational AMV algorithms. A common QI module, based on National Oceanic and Atmospheric Administration's (NOAA) implementation of the EUMETSAT QI process, was made available so that all AMV producers could implement it as part of their algorithms. EUMETSAT implemented it in the MSG AMV algorithm in the release 2.7 of the Meteosat Meteorological Product Extraction Facility (MPEF) ground segment in November 2018. The AMV output file currently contains three quality indicators for each AMV: The usual EUMETSAT QIs with and without forecast check, as well as the new common QI. The next ground segment release 2.8, foreseen in autumn 2019, will include the implementation of the new AMV BUFR sequence that was adopted by WMO in November 2018. This new sequence grants possibilities to fill the output file with new parameters on cloud properties and with diagnostic information that can be useful for the assimilation of AMVs in NWP models.

The RSS delivers rapid scan, high rate SEVIRI image data and a selection of advanced meteorological products from a position at 9.5° east. The upper third part of the nominal Earth disk is scanned every five minutes, which is similar to the frequency of ground weather radars. The high repeat cycle imagery of RSS is important for nowcasting activities and for the observation of high-impact weather events. Certain EUMETSAT users have recently requested to extend the MPEF RSS processing area of AMV production from 33.0 to 21.5 degrees north. The extension of the RSS processing area was made operational in June 2018 using *Meteosat-9* satellite data. The Canary Islands and a larger part of North Africa are now included in the new RSS processing area, and more AMVs can now be used in mesoscale NWP data assimilation. Figure 2 illustrates the RSS AMV production area before (left) and after (right) the change for AMVs extracted from *Meteosat-9* on 15 September 2018 at 12:30 UTC.

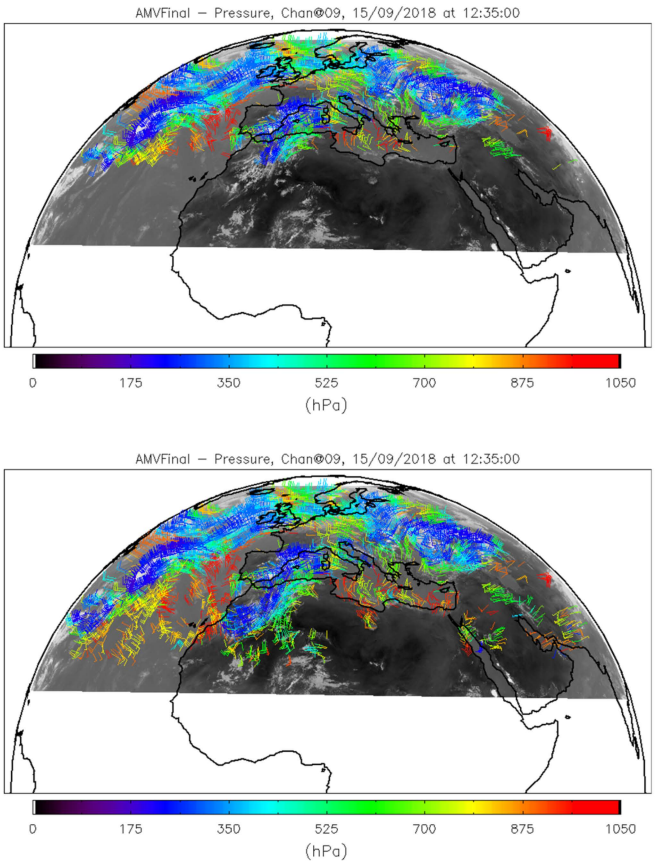


**Figure 2.** Illustration of the extension of the Rapid Scan Service (RSS) AMV production area from 33.0 (top) to 21.5 (bottom) degrees north. AMVs extracted from *Meteosat-9* on 15 September 2018 at 12:30 UTC.

### *2.2. Metop/AVHRR AMV Products*

The last satellite of the EUMETSAT Polar System program, *Metop-C*, was launched on 7 November 2018 and injected on a low polar orbit at 817 km altitude. Following the first two satellites *Metop-A* and *Metop-B*, *Metop-C* covers the same mid-morning orbit of the Joint Polar System agreement signed between EUMETSAT and NOAA, thus providing users with more frequent global-coverage observations. The first single Metop AVHRR wind products were extracted from *Metop-C* on 4 December 2018, as presented in Figure 3. The dissemination of *Metop-C* AVHRR wind products with operational status started on 14 March 2019, after the commissioning phase. The three satellites now operate in unison and will stay operating together for as long as *Metop-A's* capabilities are able to benefit the user community.

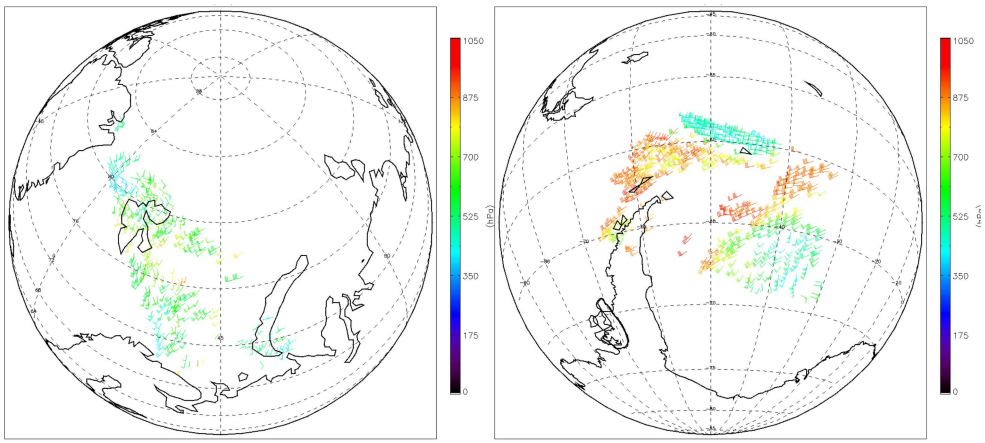


**Figure 3.** First single AVHRR AMVs extracted with *Metop-C* data the 4 December 2018 at 13:21 UTC over the northern polar region (left) and at 14:03 UTC over the southern (right) polar region.

*Metop-A* started to drift on its orbit in August 2018. In early 2019, the three satellites reached the so-called tristar configuration, with a phasing around 120 degrees between each pair of satellites along the orbit, providing new capabilities for the extraction of dual-platform Metop winds. The two complementary dual products *Metop-A/B* and *Metop-B/A* that ensured global coverage [6] were replaced on 17 January 2019 by three products extracted from the *Metop-A/B*, *Metop-B/C* and *Metop-C/A* pairs. The nomenclature *Metop-A/B* means that a pair of images taken consecutively by *Metop-B* and then by *Metop-A* has been used to extract the wind vectors, with the latest image being the reference for the wind vectors. The overall global AVHRR wind production has increased by 50%, and all wind products using *Metop-C* have been found of the same quality as the corresponding wind products extracted from the *Metop-B* and *Metop-A* satellites. However, a detailed analysis has shown that the dual-Metop AMV characteristics depend on which satellite pair is used (see Figure 4). These differences are primarily found in the tropics, where the winds extracted from the pair *Metop-A/B* have a slightly worse quality, larger speed biases, and larger root mean square (RMS) than the two other products extracted from pairs *Metop-B/C* and *Metop-C/A*. These differences are currently not fully understood but might be linked to the smaller overlapping area observed for the pair *A/B*. Indeed, since AVHRR pixel sizes vary from 1 km at their nadir to around 4 km at the edge of the swath, the overlap rate is known to be an important criterion in the wind retrieval quality.

The continuous drift of *Metop-A* in its orbit since August 2018 has modified the overlap area observed by *Metop-A* and the other Metop satellites, making the operations of AVHRR winds from multiple satellites difficult when *Metop-A* is involved. The operating production procedures need frequent updates to maintain a reliable production and a consistent dual-wind product quality. If *Metop-A* is removed from operations, the operational production of global and triplet-mode AVHRR wind products will then rely on the remaining pairs *B–C* and *C–B* only. During the *Metop-C* commissioning period, the phasing between *Metop-B* and *Metop-C* was around 120 degrees; however, two options, namely the tristar configuration (120 degrees phasing) and the trident configuration (180 degrees phasing), have been considered for the mid-term operation of the Metop satellites. These different configurations affect the coverage of the instruments on board the Metop satellites, which has an impact on both the production and the quality of AVHRR winds—see Table 1.

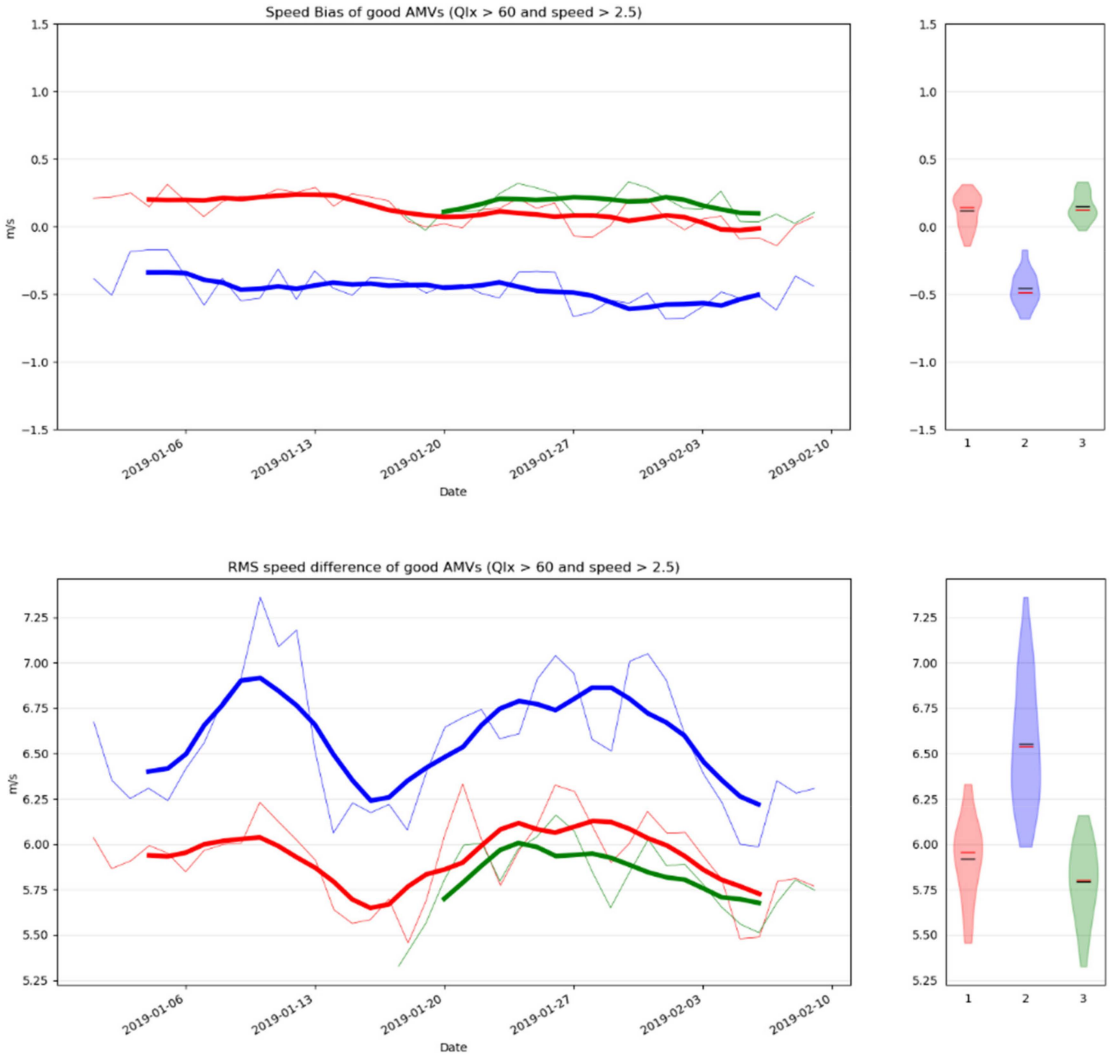


**Figure 4.** AMV speed biases (top) and root mean square (RMS) (bottom) against forecast for the dual Metop wind products extracted from *Metop-A* (red), *Metop-B* (blue) and *Metop-C* (green) over the northern region for January 2019. Only AMVs with a quality index larger than 60 and a speed larger than 2.5 m/s have been considered in the statistics. Operational change including *Metop-C* occurred the 17th January.

As it is not possible to directly compare the phasing configurations at 120° and 180° for the same day, the coverage and production of dual-Metop wind products have been compared for the pairs *A–B* and *B–A* on 21 June 2015, when *Metop-A* and *Metop-B* were in opposition (180°), and the pairs *B–C* and *C–B* on 25 February 2019, when *Metop-B* and *Metop-C* were separated 120° along the orbit. The characteristics of the two configurations are very similar regarding the overall coverage (~93%) and the amount of winds. However, as illustrated in Figure 5, the tristar configuration produces asymmetric complementary products using the pairs *B–C* and *C–B*, because the temporal gaps of each pair are 70 and 35 min, respectively, directly impacting the overlap area of the consecutive overpasses. The percentage of "good quality winds" (QI > 60) is also impacted, being a bit larger for the shorter time difference of pair *B–C* (~57%) than for pair *C–B* (~50%).

**Table 1.** Impact of *Metop-B/C* phasing on dual AVHRR wind products.

| | ***Metop-B/C* Phasing at 120°** | ***Metop-B/C* Phasing at 180°** |
|---|---|---|
| **Coverage** | - Global coverage using complementary *B–C* and *C–B* pairs.<br>- Global *C–B* products cover 50% more area than *B–C*. | - Global coverage using complementary *B–C* and *C–B* pairs.<br>- Almost equivalent coverage of the two products in the dataset. |
| **Temporal gaps** | - Asymmetric for pair *B–C* (~70 min) and pair *C–B* (35 min)<br>- Asymmetric between consecutive pairs *B–C* (~70 min) and pair *C–B* (35 min) used for triplet mode.<br>- Asymmetric between triplet mode products *B/C/B* and *C/B/C*. | - Symmetric for *B–C* and *C–B* pairs, 50 min separation between images.<br>- Symmetric separation between consecutive pairs *B–C* and *C–B* used for triplet mode. |
| **Quality** | - Quality slightly different for *B–C* and *C–B* pairs due to the different temporal gaps and the different overlap. | - Quality similar for *B–C* and *C–B*. |
| **Stability of production** | - Stable for *B–C* and *C–B* pairs. | - Stable for *B–C* and *C–B* pairs. |

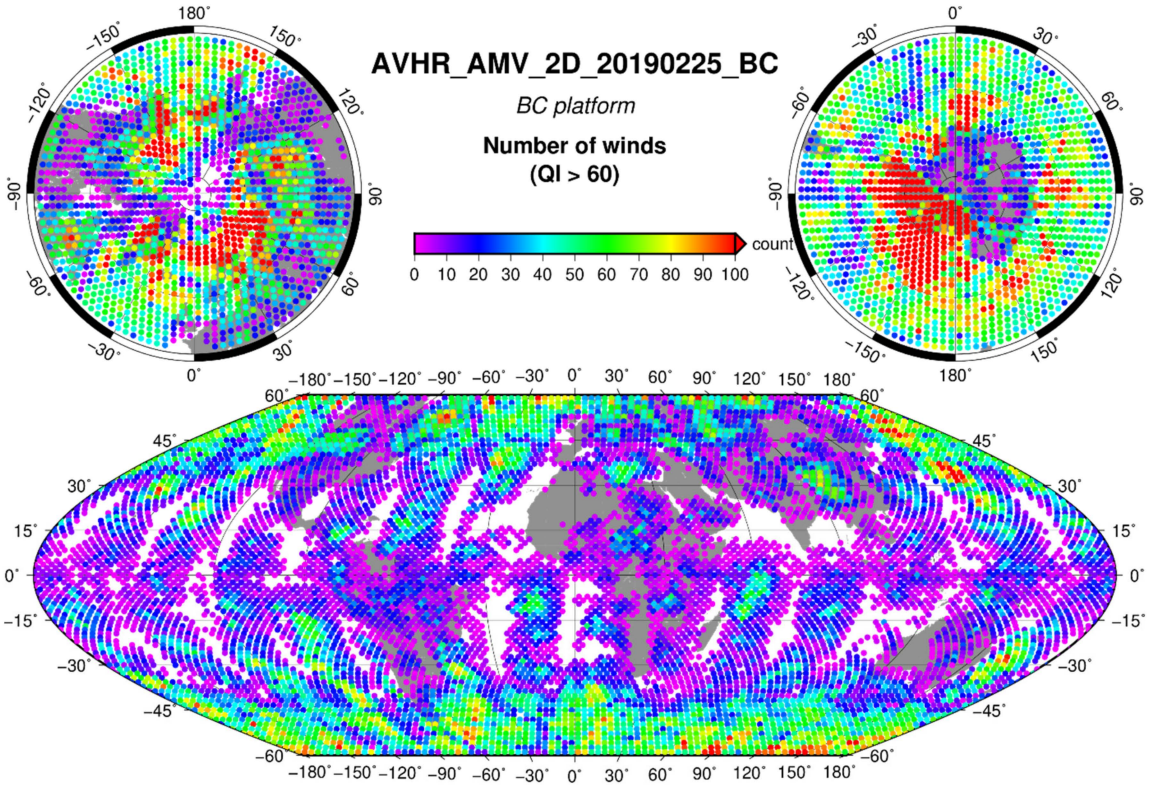


**Figure 5.** *Cont.*

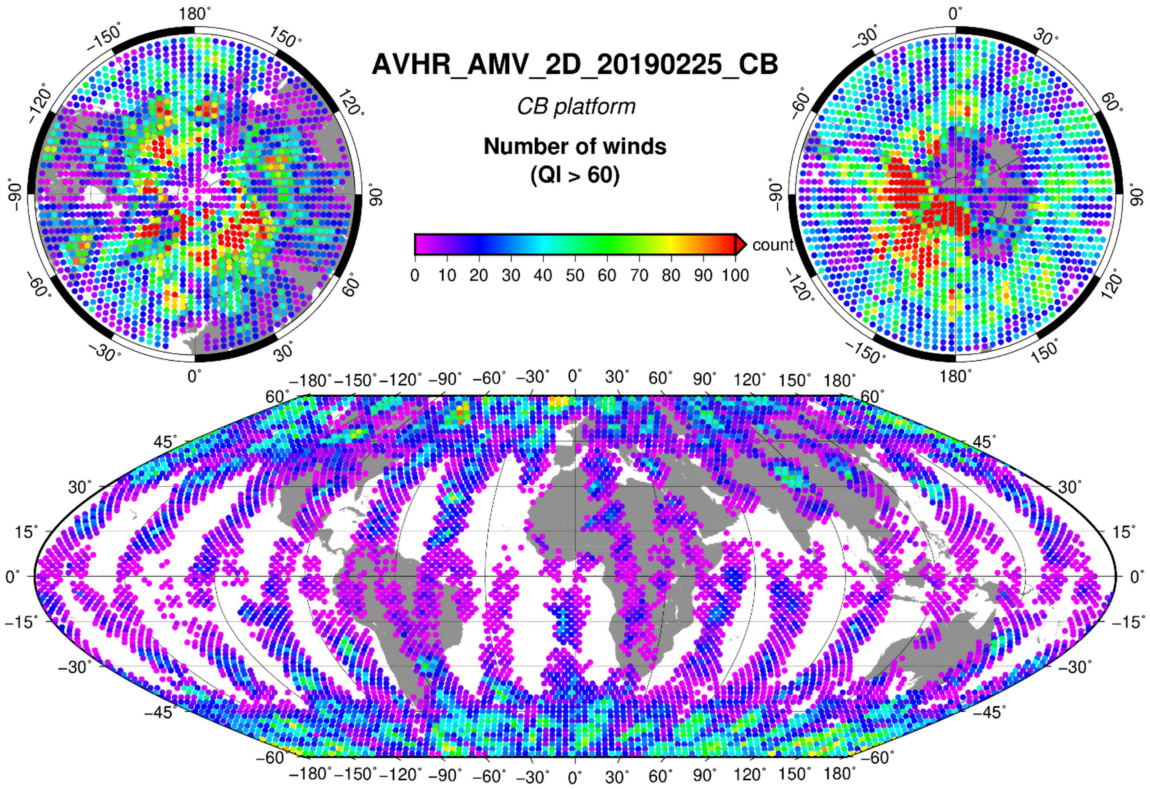


**Figure 5.** Dual-Metop wind production considering pairs *B*–*C* (top) and *C*–*B* (bottom) on 25 February 2019, illustrating the asymmetric production of the two pairs.

## 3. Upcoming AMV Extraction Capabilities at EUMETSAT

### *3.1. Preparation of MTG/FCI Prototype Code*

Table 2 illustrates the main differences between MSG/SEVIRI and MTG/FCI characteristics that are important for AMV extraction. The overall AMV production will be very similar for MTG/FCI and MSG/SEVIRI, thus ensuring the continuity of operations. The channels used for the AMV extraction and the area of AMV production will be very similar to those of MSG, with the addition of a test on AMV extraction from channel IR3.9 during nighttime. The smaller pixel size and the shorter temporal gap between consecutive images are expected to provide smaller scale observations. The MTG/FCI AMV algorithm developed at EUMETSAT is largely based on the operational MSG AMV extraction scheme [3]. However, the following differences have been considered:

(1) The MTG/FCI algorithm uses three images (at HH:15, HH:30 and HH:45) instead of the four images for MSG (at HH:00, HH:15, HH:30 and HH:45); the reference image is the one taken at HH:30 (with backward and forward tracking) instead of HH:00 (only forward tracking).
(2) No intermediate product averaging is performed to estimate the final MTG/FCI AMV product because the second intermediate component being used as final product instead.
(3) The final AMV coordinates are set to the position of the tracked feature instead of the target.

The use of only three images to derive AMVs with the MTG/FCI algorithm and the removal of the averaging process used to set the final product characteristics are expected to provide more instantaneous information on the wind vectors, which is more suitable for the smaller-scale evolution of NWP models. It also allows the user community to derive a half-hourly product that is more appropriate for assimilation in regional forecast models.

**Table 2.** Differences between MSG (Meteosat Second Generation)/SEVIRI (Spinning Enhanced Visible and InfraRed Imager) and Meteosat Third Generation (MTG)/FCI (Flexible Combined Imager) AMV product characteristics.

| | MSG/SEVIRI | MTG/FCI |
|---|---|---|
| **Spatial resolution** | 3 km (nadir) | 1 km (nadir) |
| **Temporal gap** | 15 min | 10 min |
| **Number of images used** | 4 | 3 |
| **Channels used for AMV** | VIS0.8, WV6.3, WV7.3, IR10.8 | VIS0.8, WV6.3, WV7.3, IR3.9, IR10.5 |
| **AMV Height Assignment** | CLA Cloud Product | OCA Cloud Product |
| **Coverage (GEO disk)** | <70 degrees latitude | <70 degrees latitude |
| **Product availability** | Hourly | Half hourly |

The impact of the changes proposed for the MTG/FCI AMV extraction algorithm on AMV production and quality has been studied using one month of MSG data (14 May–14 June 2016), and the results are summarized in an EUMETSAT internal report [20]. The comparison of the MSG and MTG AMV algorithms has been done on the full disk of MSG considering AMVs extracted from the VIS0.8, WV6.2, WV7.3 and IR10.8 channels. Four different configurations of the MTG/FCI algorithm have been considered for the IR10.8 channel, using 12 × 12, 16 × 16, 20 × 20 and 24 × 24 target boxes, respectively. The operational MSG software has been run for the same period and using the same dataset for two configurations: 12 × 12 and 24 × 24 target boxes. A target-box size of 24 × 24 pixels has been considered for all the other channels. The Optimal Cloud Analysis (OCA) product [21] has been used to set the AMV altitude in all cloudy target cases. The background wind guess has not been used to guide the tracking of AMVs. The AMV production using 24 × 24 target boxes for the VIS0.8 and IR10.8 channels increased by around 12% and 8%, respectively, using the MTG/FCI algorithm with respect to the MSG algorithm. The increase occurs mainly at low and mid-levels (+19.6% and +14.6% for VIS0.8, and +13.7% and 16.7% for IR10.8). The AMV production using the WV channels is very similar for both algorithms. Collocated MSG/SEVIRI and MTG/FCI AMVs have been compared within boxes of 0.05 degrees latitude and longitude, considering only speed values larger than 2.5 m/s and QI values larger than 80%. A very good agreement has been found for all the tested AMV characteristics: Speed, direction, and pressure. Statistics on the collocated AMV histogram differences showed a mean speed difference of almost 0 m/s and an associated standard deviation smaller than 1 m/s, a mean direction difference almost null with the standard deviation ranging from 3 to 6 degrees, and a mean pressure difference smaller than 1 hPa in absolute value with the standard deviation ranging from 1 to 18 hPa.

The performances of the MSG/SEVIRI and MTG/FCI algorithms have been estimated against the ECMWF NWP model forecast wind following the Coordination Group for Meteorological Satellites (CGMS) criteria used by all AMV producers to monitor the quality of AMV algorithms: A horizontal distance smaller than 150 km, a vertical distance smaller than 25 hPa, and a speed larger than 2.5 m/s. Figure 6 shows the vertical distribution of AMV speed bias and normalized root mean square (NRMS) obtained for the MSG/SEVIRI and MTG/FCI AMVs against the corresponding forecast fields. Performances for channels VIS0.8, WV6.2 (cloudy), WV7.3 (cloudy) and IR10.8 are presented from top left to bottom right. The distributions of speed biases and NRMS for the MSG/SEVIRI and MTG/FCI algorithms are very similar for all channels, with the MTG/FCI AMV speed bias values being slightly smaller in general. In [20], more detailed statistics, split by geographical area (global, northern hemisphere, southern hemisphere and tropics) and altitude level (high, mid and low), show the same trends (not shown here).

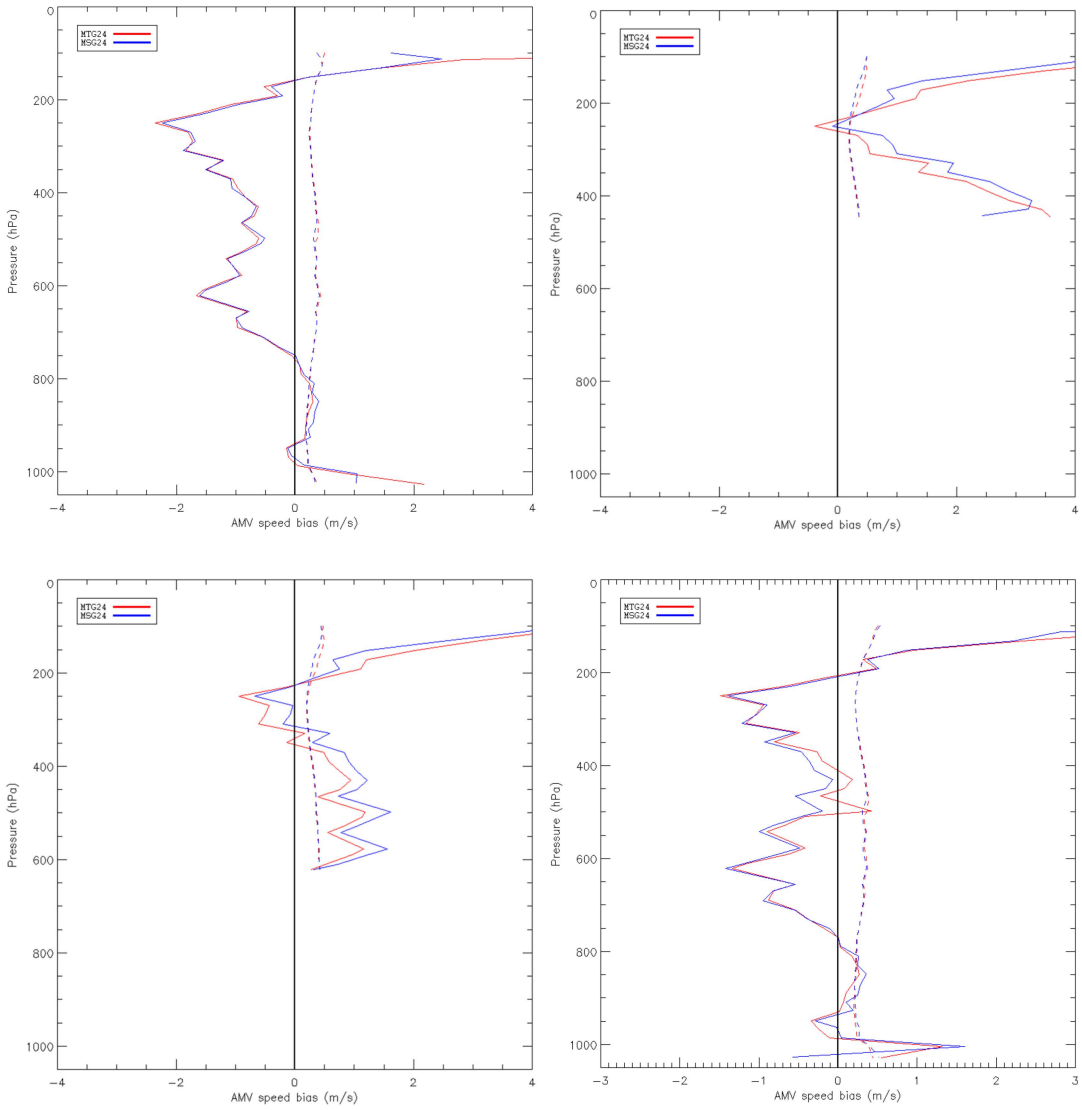


**Figure 6.** Vertical distribution of AMV speed bias (solid line) and normalized root mean square (NRMS) (dashed line) for the MSG/SEVIRI (blue) and MTG/FCI (red) algorithms using the VIS0.8 channel (top left), the cloudy AMVs from the WV6.2 channel (top right), the cloudy AMVs from the WV7.3 channel (bottom left), and the IR10.8 channel (bottom right). MSG data from 14 May to 14 June 2016 were used for these plots.

The recent evolution of global and regional forecast models requires the assimilation of smaller-scale observations in order to improve forecast scores. Several ways have been investigated to extract smaller-scale wind information by using rapid-scan imagery or smaller tracer sizes. Garcia-Pereda and Borde (2014) [22] studied the impact of the target-box size on the extraction of AMVs using MSG/SEVIRI images. They showed that the larger the tracer size, the easier the matching, because large target boxes contain a generally good contrast and entropy to select a good tracer. The proportion of good-quality winds (QI > 80) was then found logically larger for large target boxes—58.3% for MTG/FCI 24 × 24—than for small target boxes—52.5% for MTG/FCI 12 × 12. In agreement with previous studies [22,23], AMVs derived using small target boxes tend to be, on average, faster than those generated using larger target boxes, resulting in a reduction of the speed bias against forecast when the speed bias is negative (see Figure 7). The global average speed bias is, in general, negative, except at low levels, which means that AMVs are placed slightly too low in the troposphere. Geographically, the

average speed bias was mostly negative in the northern hemisphere (except at mid-levels), positive in the tropics, and negative in the southern hemisphere for the studied period.

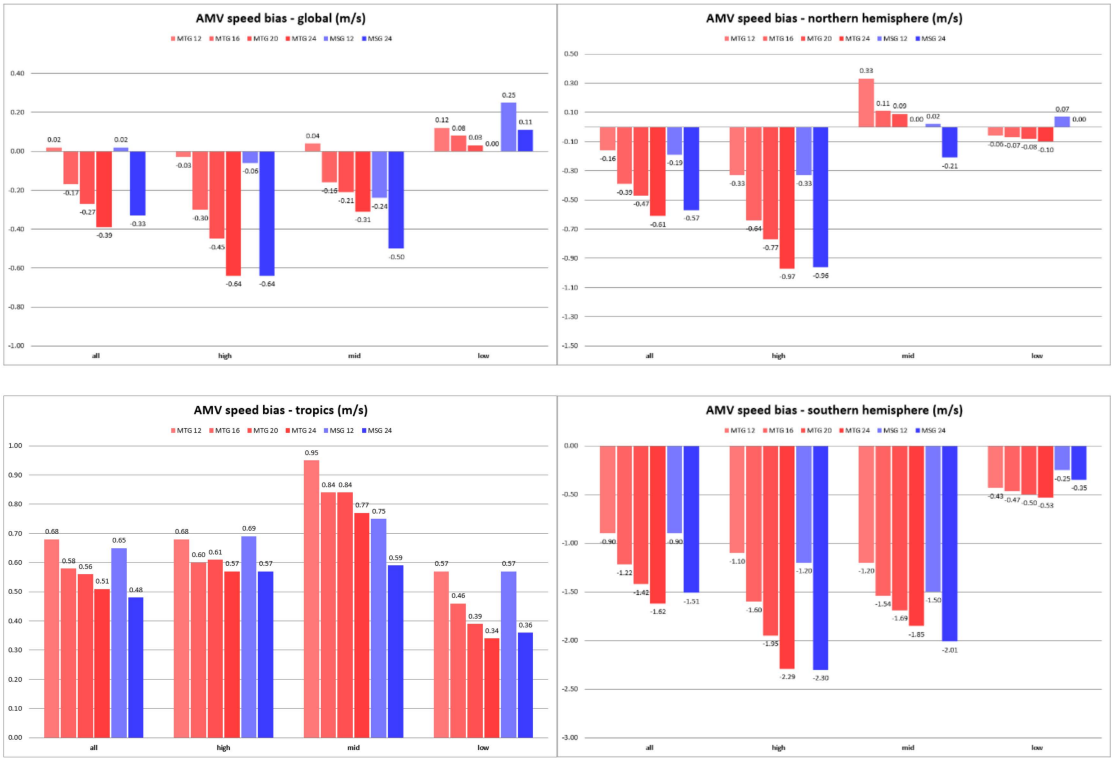


**Figure 7.** Channel IR10.8 AMV speed bias against forecast for the MSG/SEVIRI (blue) and MTG/FCI (red) algorithms, global (top left,) northern hemisphere (top right), tropics (bottom left) and southern hemisphere (bottom right), from 14 May to 14 June 2016 (QI > 80).

As a conclusion of this study, the AMV speed statistics against forecast were very similar for both MSG/SEVIRI and MTG/FCI schemes, with slightly smaller values for the MTG/FCI algorithm on average. The use of four images and the averaging process implemented within the MSG/SEVIRI algorithm did not show a significantly positive impact. These results validate the strategy planned for the operational MTG/FCI AMV processor: The AMV final product will be based on the second intermediate component, providing more instantaneous information of the wind field. Moreover, the MTG/FCI AMV algorithm will be more similar to the AMV extraction schemes already used for the AVHRR instrument at EUMETSAT and by other agencies.

### *3.2. Preparation of EPS-SG/METImage Prototype Code*

The current EUMETSAT Polar System will be replaced in the early 2020s by the so-called EPS Second Generation (EPS-SG). AMVs over the polar areas will then be extracted from the optical imager METImage on board the first Metop-SG satellite. Due to the artefacts in the images scanned by a whiskbroom instrument, some pixels can be seen twice on different line scans. Therefore, the extraction of AMV products from METImage data requires a previous correction of this so-called "bow-tie effect." This purely geometric effect needs to be corrected for AMV products because they require an accurate positioning, viewing angle and solar zenith angle for each pixel. The consecutive images used for the AMV extraction need to be accurately positioned on a grid in order to correctly estimate the motion of cloud features from the first to the second image. A tool has been developed at EUMETSAT [24] based on the Ground Track Oblique Cassini (GTOC) projection, which is well suited for sensors like METImage [25]. The GTOC algorithm includes the Earth-to-map transformation, which is missing in the ground track Mercator projection. It then provides the transformation from latitude/longitude

to mapping space and vice versa, and it suppresses the bow-tie effect in one go. Furthermore, the pixel distortion seems very small and occurs only in one direction when the pixel is away from the ground track.

Once the image data are projected on the grid, the core AMV extraction processing used for METImage is similar to the algorithm proposed for MTG/FCI, however, as it only uses two images for the dual AVHRR wind products. The temporal consistency test between the two consecutive intermediate vectors that are obtained using image triplets cannot be performed using only image pairs. Therefore, a 'reverse' matching is realized to assess the quality of the first tracking, as described by Hautecoeur and Borde, 2017 [4] for the AVHRR AMV extraction algorithm. Table 3 summarizes the expected improvements of the EPS-SG METImage AMV production compared to the current Metop AVHRR winds. The spatial resolution will be improved with METImage with respect to AVHRR, from 1 km at its nadir to 500 m. The temporal gap between consecutive images cannot be reduced, as it depends on the orbital parameters and will remain identical at around 100 min when using data from only one satellite for the wind extraction. The most significant improvement will come from the extraction of AMVs from one visible and two water-vapor channels. The extraction of water-vapor winds from LEO satellites over polar areas is a high-level requirement from the user community that is presently ensured by the MODIS instrument on board the NASA EOS-TERRA and EOS-AQUA missions. METImage is expected to take over the water-vapor winds production capability over polar areas after 2022. The use of a cloud properties product to set the AMV altitude will also improve the overall quality of the polar wind products. The MOCA product developed for METImage is based on the same optimal estimation process [21] used for the MTG/FCI cloud product at EUMETSAT.

**Table 3.** Differences between EPS/AVHRR and EUMETSAT Polar System-Second Generation (EPS-SG)-METImage AMV products characteristics.

| | **AVHRR** | **METImage** |
|---|---|---|
| **Spatial resolution** | 1 km (nadir) | 500 m (nadir) |
| **Temporal gap** | 50 min | 50 min |
| **Channels used for AMV** | IR10.8 | VIS0.6, IR3.7, WV6.3, WV7.3, IR10.8 |
| **AMV Height Assignment** | EBBT + IASI | Cloud Product |
| **Coverage single spacecraft** | >50 degrees latitude | >50 degrees latitude |
| **Coverage tandem operations** | Global | Global |
| **Single-satellite product availability** | Every 100 min | Every 100 min |

The launch of *Metop-SG-A* is presently planned for Autumn 2022, and the algorithm prototyping activities for the METImage instrument are ongoing and using the algorithm baselines developed for EPS/AVHRR and MTG/FCI. The scientific validation of METImage AMVs is planned to be performed against global performances of similar polar wind products extracted from MODIS, VIIRS and AVHRR.

### *3.3. Preparation of SENTINEL-3 SLSTR Prototype Code*

As mentioned above, the continuity of AMV production over high-latitude areas (poleward of 60 degrees) will be ensured by the METImage instrument, but a single LEO satellite cannot populate the 50–70 degree latitude band with AMV observations. The sustainability of this capability will be ensured by the two Sentinel-3 Sea and Land Surface Temperature Radiometer (SLSTR) instruments presently in orbit used in dual mode. The SLSTR instrument is a conical-scanning imaging radiometer with an along-track scanning dual-view capability providing a swath coverage of around 740 km for the oblique view and around 1400 km for the nadir view. Considering the similarities between the AVHRR and SLSTR instruments, the AMV extraction algorithm for S3/SLSTR is very close to the Metop/AVHRR polar wind algorithm. The main difference regarding the production comes from the narrower SLSTR swath (about half of the AVHRR swath), which reduces the AMV production area, as seen in Table 4. With the launch of *Sentinel-3B* in 2018, two SLSTR instruments are now in orbit. The SLSTR algorithm can be configured for the extraction of "dual" wind products (using two or three

images) and is similar to the current global AVHRR approach. Global coverage cannot be expected due to the smaller swath of SLSTR, but AMV extraction should be possible poleward of around 35–40 degrees latitude. The design of the S3/SLSTR AMV extraction algorithm considers only the nadir view swath to ensure a good coverage of the AMV production. The use of the limited 740 km oblique view swath does not allow for AMV extraction in the 50–70 latitude bands using consecutive images taken from the two satellites. However, the oblique view could be used later, in a second step, for the validation and monitoring of the AMV product quality.

**Table 4.** Upcoming Sentinel-3 Sea and Land Surface Temperature Radiometer (S3/SLSTR) AMV product characteristics.

| | **SLSTR** |
|---|---|
| **Spatial resolution** | 1 km (nadir) |
| **Temporal gap** | 40/60 min |
| **Channel used for AMV** | IR10.8 |
| **AMV Height Assignment** | EBBT or Cloud product |
| **Coverage Single spacecraft** | >70 degrees latitude |
| **Coverage Tandem operation** | >40 degrees latitude |
| **Single-satellite product availability** | Every 100 min |

Input data and products considered in the process are projected on a fixed equal-area grid before the tracking step [24]. Figure 8 shows an example of AMVs extracted from a pair of SLSTR images taken over the Arctic Ocean on 4 July 2018 at 15:53:21 UTC and 17:34:20 UTC. The color scale represents the AMV altitude. The operational production of S3/SLSTR AMVs at EUMETSAT is currently foreseen for the end of 2020.

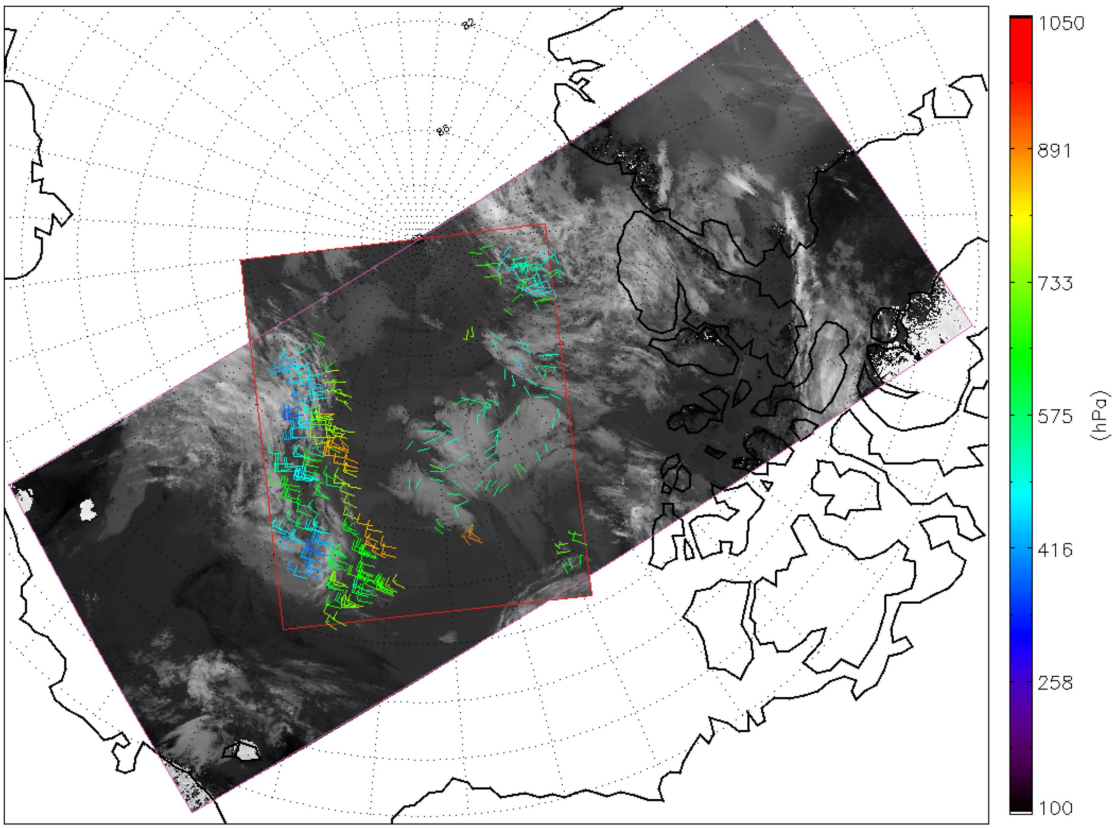


**Figure 8.** AMVs extracted from SLSTR images taken over the Arctic Ocean on 3 July 2019 at 02:09:49 UTC (red contour) and from 00:25:50 to 00:34:50 UTC (purple contour).

### *3.4. 3D Winds from IR Sounders*

Several studies have been conducted by EUMETSAT to investigate the extraction of wind profiles from moisture and temperature fields retrieved from hyperspectral instruments [11,12]. These studies have demonstrated technical feasibility, but they have also pointed out difficulties and limitations linked to the common techniques used to extract AMVs and the characteristics of the moisture fields used, which are derived from IR sounders. Most of the AMV extraction algorithms apply cross-correlation technics on sequences of consecutive images. The frequent lack of contrast in the moisture fields retrieved from IR sounders does not permit the unambiguous identification of features in the images. This frequently leads to a poor matching, limiting overall AMV production. If the individual AMVs extracted are found with good quality, the winds obtained are very sparse, and they do not represent wind profiles (i.e., obtaining wind characteristics at several levels in the atmosphere at the same geographical location).

A 3D optical-flow scientific processor has been adapted from Héas and Mémin, 2008 [14] to ingest IASI level 2 humidity, ozone and temperature profiles. Wind profiles are retrieved from pairs of IASI datasets taken consecutively by the *Metop-A* and *Metop-B* satellites over high-latitude areas. Humidity profiles are mostly used as tracers in the lower part of the troposphere, whereas the ozone profiles are preferred in the higher troposphere and low stratosphere. Horizontal wind profiles are retrieved on isobaric surfaces from the ground up to 10–20 hPa altitude. It is beyond the scope of this paper to describe in detail the algorithm developed at EUMETSAT to extract 3D wind profiles from hyperspectral sounders. A specific paper is currently in preparation.

A one-month demonstration period (June 2017) has been made available to the user community. Though in a preliminary stage, the first results look very promising, providing dense wind fields at 19 levels in the atmosphere over areas poleward of 45 degrees using IASI data, as seen in Figure 9. New developments are presently ongoing at EUMETSAT to provide a quality index associated to each 3D IASI wind in order to filter out the outliers and enable the potential use of these new products in assimilation. The operational production of the 3D IASI wind demonstration product is foreseen for the second part of 2020. The algorithm will then be adapted to process operationally EPS-SG/IASI-NG level 2 products around 2024. However, the main objective for the extraction of 3D winds is the MTG/IRS instrument on board the MTG-S satellites, the first of which is planned to be launched in 2023. The full geo disc is divided into four local area coverage (LAC) zones that corresponds each to an area which can be scanned in 15 min by the MTG-IRS instrument. The current six hour scanning baseline of the four LAC zones [3-4 3-4 3-4 3-4 3-4; 2-4 2-4 2-4 2-4; and 1-4 1-4 1-4] planned for the MTG/IRS instrument should allow for the frequent observation of the LAC4, which covers Europe with a sub satellite pixel sampling of 4 k, and allows for the production of 3D winds every 30 min over this area. This could be a major step forward in the observation of atmospheric dynamics from satellite data.

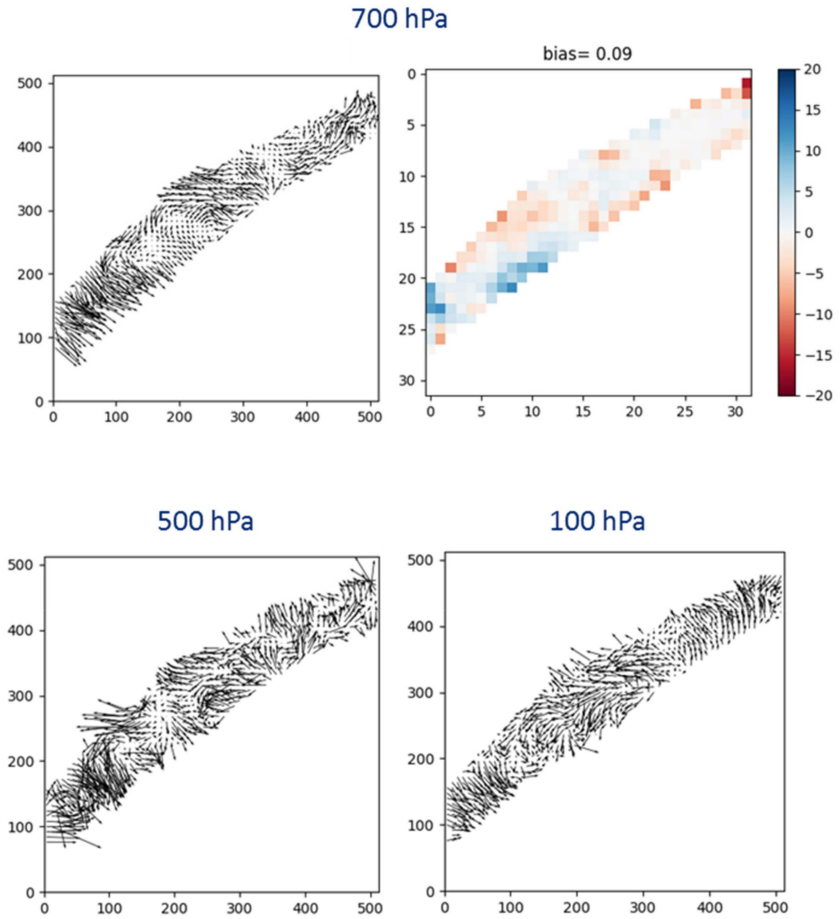


**Figure 9.** Example of 3D Infrared Atmospheric Sounding Interferometer (IASI) winds extracted at 700, 500 and 100 hPa from *Metop A* and *Metop B* consecutive orbits over northern polar areas on 4 July 2018 at 00:46:09 UTC. Speed bias against forecast fields is shown for the 700 hPa retrieval. Data are projected on polar stereographic grid centered on North Pole and have a nominal resolution of 20 km. X and Y axis units correspond to grid coordinates.

## 4. Conclusions

This paper presents an overview of the current and upcoming AMV extraction capabilities at EUMETSAT. The EUMETSAT contribution to the global AMV production should be increased with the new generations of geostationary and low-orbit polar satellites that are going to be launched in 2021 and 2023, respectively. Taking advantage of the better characteristics of the new instruments on board, both the total amount of winds extracted and their individual quality are expected to improve. The capability to extract AMVs from the two water-vapor channels of the EPS-SG METImage instrument over high-latitude regions is seen as especially critical by the user community in order to replace the current water-vapor AMVs production from MODIS.

Besides the improvements expected from the new generation of satellites, EUMETSAT plans to produce operational AMVs from the S3/SLSTR instruments. These winds should complement the current polar wind production from AVHRR and help to fill the gap of wind observations in the 40–60 latitude bands during the transition period between the EPS and EPS-SG programs. Finally, although still under development at EUMETSAT, the recent results on the extraction of 3D wind profiles from infrared sounders should allow EUMETSAT to plan the operational production with both the EPS-SG/IASI-NG and MTG/IRS instruments by 2024. This could potentially provide a significant improvement in the observation of atmospheric dynamics from satellite data in the next decade.

**Author Contributions:** Conceptualization and supervision, R.B.; methodology, R.B., O.H. and M.C.; software, O.H., M.C. and K.B.; validation, R.B., O.H., M.C. and K.B.; formal analysis, R.B., O.H., M.C. and K.B.; writing—original draft preparation, R.B.; writing—review and editing, R.B., O.H., M.C. and K.B.

**Funding:** The work was totally supported by the European Organization for the Exploitation of Meteorological Satellites (EUMETSAT).

**Acknowledgments:** Authors wish to thank INRC team from EUMETSAT RSP division, and especially M. de Bartolomei, for the provision of the reprojection tool software that allows derivation of AMVs from EPS-SG METImage and S3-SLSTR instruments. Authors also wish to thank ECMWF for their ECMWF satellite data monitoring website which allowed production of the plots of the Figure 1.

**Conflicts of Interest:** The authors declare no conflict of interest.

## References

1. English, S.; McNally, T.; Bormann, N.; Salonen, K.; Matricardi, M.; Horanyi, A.; Rennie, M.; Janisková, M.; Di Michele, S.; Geer, A.; et al. *Impact of Satellite Data*; ECMWF Research Department Techn. Memo. 711; ECMWF: Reading, UK, October 2013; Available online: https://www.ecmwf.int/sites/default/files/elibrary/2013/9301-impact-satellite-data.pdf (accessed on 20 May 2013).
2. Yoshiaki, S.; Riishojgaard, L.P. Workshop Report "Sixth WMO Workshop on the Impact of Various Observing Systems on Numerical Weather Prediction", Shanghai, China, 10–13 May 2016. WMO: Geneva, Switzerland. Available online: https://www.wmo.int/pages/prog/www/WIGOS-WIS/reports/WMO-NWP-6_2016_Shanghai_Final-Report.pdf (accessed on 19 June 2016).
3. Borde, R.; Doutriaux-Boucher, M.; Dew, G.; Carranza, M. A Direct Link between Feature Tracking and Height Assignment of Operational EUMETSAT Atmospheric Motion Vectors. *J. Atmos. Oceanic Technol.* **2014**, *31*, 33–46. [CrossRef]
4. Hautecoeur, O.; Borde, R. Derivation of wind vectors from AVHRR Metop at EUMETSAT. *J. Atmos. Ocean. Technol.* **2017**, *34*, 1645–1659. [CrossRef]
5. Horváth, Á.; Hautecoeur, O.; Borde, R.; Deneke, H.; Buehle, S.A. Evaluation of the EUMETSAT Global AVHRR Wind Product. *J. Appl. Meteor. Climatol.* **2017**, *56*, 2353–2376. [CrossRef]
6. Borde, R.; Hautecoeur, O.; Carranza, M. EUMETSAT Global AVHRR winds product'. *J. Atmos. Oceanic Technol.* **2016**, *33*, 429–438. [CrossRef]
7. *Metop-C AVHRR Winds Product Validation Report*; EUMETSAT Internal Report EUM/RSP/TEN/19/1053059; EUMETSAT: Darmstadt, Germany, 2019.
8. Key, J.; Santek, D.; Velden, C.S.; Bormann, N.; Thepaut, J.-N.; Riishojgaard, L.P.; Zhu, Y.; Menzel, W.P. Cloud-drift and Water Vapor Winds in the Polar Regions from MODIS. *IEEE Trans. Geosci. Remote Sens.* **2003**, *41*, 482–492. [CrossRef]
9. De Haan, S.; Stoffelen, A. Assimilation of High-Resolution Mode-S Wind and Temperature Observations in a Regional NWP Model for Nowcasting Applications. *Weather Forecast.* **2012**, *27*, 918–937. [CrossRef]
10. EUMETSAT. *HQ Level 2 Products Generation and Dissemination Baseline for MTG*; EUMETSAT Internal Document EUM/MTG/DOC/09/0026; EUMETSAT: Darmstadt, Germany, 2013.
11. Mannstein, H.; Bugliaro, L.; Keil, C.; Zinner, T. *2006 Derivation of Atmospheric Motion Vectors from Forecast Model Fields of Atmospheric Moisture*; Final Report EUMETSAT ITT 06/738; EUMETSAT: Darmstadt, Germany, 2006.
12. Stewart, L. Derivation of AMVs from single-level retrieved MTG-IRS moisture fields. In Proceedings of the Eleventh International Winds Workshop, Auckland, New Zealand, 20–24 February 2012.
13. Santek, D.; Daloz, A.S.; Tushaus, S.; Rogal, M.; McCarty, W. Feature-tracked 3D Winds from Satellite Sounders: Derivation and Impact in Global Models. In Proceedings of the Thirteenth International Winds Workshop, Monterey, CA, USA, 27 June–1 July 2016.
14. Héas, P.; Mémin, E. 3D motion estimation of atmospheric layers from image sequences. *IEEE Trans. Geosci. Remote Sens.* **2008**, *46*, 2385–2396. [CrossRef]
15. Hautecoeur, O.; Borde, R.; Héas, P. 3D IASI Winds Product at EUMETSAT. In Proceedings of the Fourteenth International Winds Workshop, Jeju, Korea, 23–27 April 2018.
16. Genkova, I.; Borde, R.; Schmetz, J.; Daniels, J.; Velden, C.; Holmlund, K. Global atmospheric motion vectors intercomparison study. In Proceedings of the 9th International Winds Workshop, Annapolis, MD, USA, 14–18 April 2008.

17. Genkova, I.; Borde, R.; Schmetz, J.; Velden, C.; Holmlund, K.; Bormann, N.; Bauer, P. Global atmospheric motion vector intercomparison study. In Proceedings of the 10th International Winds Workshop, Tokyo, Japan, 22–26 February 2010.
18. Santek, D.; Velden, C.; Genkova, I.; Wanzong, S.; Stettner, D.; Mindock, M.; García-Pereda, J. AMV Intercomparison Study. In Proceedings of the 12th International Winds Workshop, Copenhagen, Denmark, 15–20 June 2014.
19. Santek, D.; Dworak, R.; Nebuda, S.; Wanzong, S.; Borde, R.; Genkova, I.; García-Pereda, J.; Galante Negri, R.; Carranza, M.; Nonaka, K.; et al. 2018 Atmospheric Motion Vector (AMV) Intercomparison Study. *Preprints* **2019**. [CrossRef]
20. Borde, R.; Carranza, M. *Comparison MSG And MTG AMV Algorithms*; EUMETSAT Internal Report EUM/RSP/REP/18/1008399; EUMETSAT: Darmstadt, Germany, 2019.
21. Watts, P.D.; Bennartz, R.; Fell, F. Retrieval of two-layer cloud properties from multispectral observations using optimal estimation. *J. Geophys. Res.* **2011**, *116*, D16203. [CrossRef]
22. Garcia-Perreda, J.; Borde, R. The impact of the Tracer size and the Temporal gap between images in the extraction of Atmospheric Motion Vectors. *J. Atmos. Ocean. Technol.* **2014**, *31*, 1761–1770. [CrossRef]
23. Bresky, W.; Daniels, J.; Bailey, A.; Wanzong, S. New Methods toward Minimizing the Slow Speed Bias Associated with Atmospheric Motion Vectors. *J. Appl. Meteor. Climatol.* **2012**, *51*, 2137–2151. [CrossRef]
24. De Bartolomei, M. *Generic Projection Tool-Technical Note*; EUMETSAT Doc. EUM/RSP/TEN/18/1030434; EUMETSAT: Darmstadt, Germany, 2019.
25. Mills, S. *The Ground Track Oblique Cassini Projection Used for Producing VIIRS Mapped Imagery*; SPIE Optical Engineering + Applications: San Diego, CA, USA, 2014; Available online: https://www.spiedigitallibrary.org/conference-proceedings-of-spie/9218/92180C/The-ground-track-oblique-Cassini-projection-used-for-producing-VIIRS/10.1117/12.2060760.full?SSO=1 (accessed on 9 August 2014).